AD-A063 258 BOSTON UNIV MASS DEPT OF ASTRONOMY F/G 3/2
SYNOPTIC CHARTS OF CORONAL HOLES AND 9.1 CM SOLAR DATA FROM MAY--ETC(U)
JAN 79 F L WEFER, M D PAPAGIANNIS F19628-77-C-0189
UNCLASSIFIED SER-II-NO-68 AFGL-TR-78-0284 NL

| OF |
AD
A063258

END
DATE
FILMED
3--79
DDC

LEVEL II

(18) (19) AFGL-TR-78-0284

(12) B.S.

(6) SYNOPTIC CHARTS OF CORONAL HOLES AND 9.1 CM SOLAR DATA FROM MAY THROUGH AUGUST 1973

(10) Fred L. Wefer
Michael D. Papagiannis
Michael E. Van Steenberg
Terry M. Varner

Department of Astronomy
Boston University
725 Commonwealth Avenue
Boston, Massachusetts 02215

Scientific Report No. 2

(11) January 1979

(14) SER-II-NO-68, SCIENTIFIC-2

Approved for public release; distribution unlimited.

(12) 32 p.

(15) F19628-77-C-0189

AIR FORCE GEOPHYSICS LABORATORY
AIR FORCE SYSTEMS COMMAND
UNITED STATES AIR FORCE
HANSCOM AFB, MASSACHUSETTS 01731

(16) 2311

(17) G3

UNCLASSIFIED

SECURITY CLASSIFICATION OF THIS PAGE *(When Data Entered)*

REPORT DOCUMENTATION PAGE		READ INSTRUCTIONS BEFORE COMPLETING FORM
1. REPORT NUMBER AFGL-TR-78-0284	2. GOVT ACCESSION NO.	3. RECIPIENT'S CATALOG NUMBER
4. TITLE *(and Subtitle)* SYNOPTIC CHARTS OF CORONAL HOLES AND 9.1 CM SOLAR DATA FROM MAY THROUGH AUGUST 1973.		5. TYPE OF REPORT & PERIOD COVERED Scientific Report No. 2 6. PERFORMING ORG. REPORT NUMBER A.C.B.U., Ser. II, No. 68
7. AUTHOR(s) Fred L. Wefer, Michael D. Papagiannis Michael E. Van Steenberg, and Terry Varner		8. CONTRACT OR GRANT NUMBER(s) F-19628-77-C-0189
9. PERFORMING ORGANIZATION NAME AND ADDRESS Department of Astronomy Boston University 725 Commonwealth Ave. Boston, Massachusetts 02215		10. PROGRAM ELEMENT, PROJECT, TASK AREA & WORK UNIT NUMBERS 61102F 2311G3 BB
11. CONTROLLING OFFICE NAME AND ADDRESS Air Force Geophysics Laboratory Hanscom AFB, Massachusetts 01731 Monitor/D. Guidice/PHP		12. REPORT DATE January, 1979 13. NUMBER OF PAGES 30
14. MONITORING AGENCY NAME & ADDRESS*(if different from Controlling Office)*		15. SECURITY CLASS. *(of this report)* Unclassified 15a. DECLASSIFICATION/DOWNGRADING SCHEDULE

16. DISTRIBUTION STATEMENT *(of this Report)*

Approved for public release; distribution unlimited

17. DISTRIBUTION STATEMENT *(of the abstract entered in Block 20, if different from Report)*

18. SUPPLEMENTARY NOTES

19. KEY WORDS *(Continue on reverse side if necessary and identify by block number)*

Solar Radio Maps; Coronal Holes; Synoptic Charts

20. ABSTRACT *(Continue on reverse side if necessary and identify by block number)*

A review of the geomagnetic disturbances due to high-speed solar wind streams produced by coronal holes is given in the introduction. Also discussed is the history of radio observations of coronal holes, with special mention of some early radio results which were obtained before the unambiguous identification of coronal holes from X-ray photographs. In the main part of this work, using the central meridian column of the 9.1 cm

DD FORM 1 JAN 73 1473 EDITION OF 1 NOV 65 IS OBSOLETE UNCLASSIFIED

the authors

Stanford solar radio maps, ~~we have~~ constructed synoptic charts emphasizing temperatures near the quiet solar disk level. Synoptic charts were made for Carrington Rotations 1601-1605 (May - August 1973) which represents the overlapping period from the commencement of solar X-Ray data from ATM - Skylab (28 May 1973) to the termination of the Stanford solar radio mapping program (11 August 1973). Synoptic charts of coronal holes were superimposed on the radio charts to determine if the 9.1 cm synoptic charts could be used to identify coronal holes. Coronal Hole 1 is clearly seen as a depression in the solar emission in Carrington Rotations 1602 and 1603, while the depression produced by the coronal hole is wiped out by adjacent active regions or sidelobe effects of other active regions in Rotations 1601 and 1604. In Rotation 1603, not only can one clearly see the depression produced by CH1 but also a small active region at 10° N engulfed by the coronal hole, which is also present in the X-Ray pictures. Coronal Hole 5 is clearly seen as a depression in Rotation 1602, this being the only rotation in which CH5 was identified on the X-Ray pictures. Coronal Holes 2 and 3 were either too small or too narrow to be seen with the beam of the Stanford antenna, while CH4 had not yet appeared on the solar disk. In conclusion, the 9.1 cm synoptic charts can be of substantial value in identifying large coronal holes, especially during periods of low solar activity. Such synoptic charts, especially during the 1962-65 period of low solar activity, could strengthen the confidence on coronal hole boundaries in the 1960-1973 pre-Skylab period, which have been determined from occasional rocket X-Ray photographs.

Their findings lead them to conclude that

SYNOPTIC CHARTS OF CORONAL HOLES AND 9.1 CM SOLAR DATA FROM MAY THROUGH AUGUST 1973

Fred L. Wefer, Michael D. Papagiannis
Michael E. Van Steenberg, and Terry M. Varner

Dept. of Astronomy, Boston University, Boston, Massachusetts 02215

1. INTRODUCTION

The ambient medium of the earth, consisting of the atmosphere, ionosphere, and magnetosphere, resides in inter-planetary space which is an extension of the solar atmosphere. It is not surprising then, that changes in the solar atmosphere have both direct and indirect effects on the earth. These effects range from variations in the ozone layer to the disruption of telecommunications, and from geomagnetic disturbances to dangerous conditions for astronauts in space. For these reasons a large effort of the solar physics community has been directed for several years in the study of the many and complex forms of solar-terrestrial relations.

That geomagnetic disturbances show a tendency to occur at approximately 27-day intervals has long been known. Satellite measurements of the solar wind have shed much light on this phenomenon. Snyder et al. (1963) showed the remarkable correlation between ΣK_p (the sum of 8, three-hour K_p values for a given day) and the solar wind velocity:

$$V \text{ (km sec}^{-1}) = 8.44\ \Sigma K_p + 330. \qquad (1)$$

Maer and Dessler (1964) showed a similar relationship between the solar wind velocity and A_p (the equivalent daily planetary amplitude index of the geomagnetic field):

$$v \text{ (km sec}^{-1}) = 290\ A_p^{0.22} . \qquad (2)$$

It was assumed that the streams of plasma responsible for the recurrent geomagnetic activity were emitted from localized regions (which had been named "M-regions") on the sun. There was, however, no strong correlation between solar activity (as indicated, for example, by the sunspot number or the 10.7 cm-λ solar flux density) and the observed solar wind velocity. The identity of the mysterious M-regions, thought to be responsible for the high speed solar wind streams, remained unknown until the 1970's.

It is now apparent that the sources of recurrent high-speed solar wind streams are the coronal holes. Krieger et al. (1973) have shown a direct correspondence in position on the solar disk of a large coronal hole (observed at soft X-Ray wavelengths from a sounding rocket) and the source of a high-speed solar wind stream. They also found agreement between the magnetic polarity of the hole and the polarity of the corresponding sector structure in the inter-planetary magnetic field.

Neupert and Pizzo (1974) studied the correlation between coronal holes (as seen in the OSO-7 284 Å heliograms) and A_p. They summarized the results of their study as follows: "Of all the solar features examined (bright coronal regions, major sunspot areas, plage areas, and coronal holes) only coronal holes of substantial size lying at least in part near the

ecliptic plane at central meridian passage (CMP) are associated with recurrent geometric activity."

Nolte et al. (1976a) showed that during the Skylab period, large near-equatorial coronal holes were invariably associated with high-speed solar wind streams near the Earth. They found that the maximum velocity of the high-speed solar wind stream was related to the area (within 10^{o} of the ecliptic plane) of the associate coronal hole by:

$$V \text{ (km sec}^{-1}) = 80 \text{ A } (10^{10} \text{ km}^2) + 426.$$

Sheely et al. (1976) made a comparison between coronal holes, solar wind streams and geomagnetic disturbances of the period 1 January 1973 through 8 February 1976. Their study revealed that long-lived patterns of the three phenomena are remarkably alike. They noted small-scale differences between the patterns, differences which they attributed to major solar flare events and to the non-radial extensions of the coronal holes into the outer corona.

Coronal holes are best observed as dark regions on the solar disk at soft X-Ray wavelengths, which is the characteristic spectral region for emission originating in the hot ($T \simeq 10^6$ K) coronal plasma. Solodyna et al. (1977) have shown that the intensity of the X-Ray emission from a coronal hole can be an order of magnitude less than the focal plane intensity from the quiet corona. Coronal holes appear as dark areas because of lower plasma densities and lower temperatures, which result in lower emission intensities. The lower plasma densities are produced by open configuration of the solar

magnetic field which not only facilitate the escape of solar plasma from the coronal hole region but most likely also form a DeLaval nozzle-like configurations which accelerate the solar wind to higher velocities.

2. RADIO OBSERVATIONS OF CORONAL HOLES

Radio radiation over a considerable wavelength range originates in the transition zone and the solar corona. Thus, it should not be surprising that coronal holes have also been observed at radio wavelengths. Probably the first radio observations of coronal holes were presented by Roosen (1969). Using data at 3.3 GHz (9.1 cm-λ) from the Stanford Radio Astronomy Institute, he constructed synoptic diagrams by averaging points at the same heliographic coordinates over 7 successive days centered on the day of CMP. Mutually independent values were obtained by selecting points separated by at least the beamwidth of the telescope. On the basis of these diagrams, Roosen (1969) concluded that the then hypothetical 'M-regions' responsible for the recurrent geomagnetic disturbances were characterized by local depressions of the 9.1 cm-λ brightness. Roosen gave three arguments to support this conclusion. (1) The time interval between the CMP of the depressions in brightness and the enhanced geomagnetic activity ($\simeq$4 days) agreed well with the interval between the CMP of certain active regions of the starts of the associated geomagnetic disturbances. This delay yielded maximum correlation with the velocities of the enhanced solar wind speed measured in interplanetary space. (2) The depressions were stable for

many solar rotations. This is a necessary condition for the identification with the long-lived M-regions. (3) The longitudinal extents of the depressions in brightness were of the same order of magnitude as the durations of the recurrent geomagnetic disturbances.

Using the polytropic solar wind model given by Parker (1963), Roosen showed that the depressions in brightness were a consequence of a considerably lower density and perhaps somewhat higher temperature of the corona in the M-regions. He suggested the name "coronal depressions" for these regions from which emerge the long-lived high-velocity solar wind streams. Roosen's pioneering work has been largely ignored.

While Roosen was the first to realize the connection between regions of depressed radio emission and recurrent geomagnetic activity, others had noted the presence of such regions. For example, in studying observations at 91 GHz (3.3 mm-λ) made with the Aerospace Corporation's 4.6 m (15 ft) antenna, Simon (1965) found that areas of enhanced radio brightness correlated very well with the Hα active regions. One feature of the radioheliograms, however, which the Hα photographs did not explain was the occurence of regions of emission lower than average. In a comparison with solar magnetograms, it was found that these areas of depressed radio emission correlated with regions of little or no magnetic field. Figure 1 shows the 3.3 mm-λ radio maps for 22 and 23 August 1964 from Simon (1965). Figure 2 shows a plot of A_p for several months on either side of these dates. It appears likely (in hindsight) that the area of reduced radio emission was associated with a recurrent geomagnetic disturbance. Were these

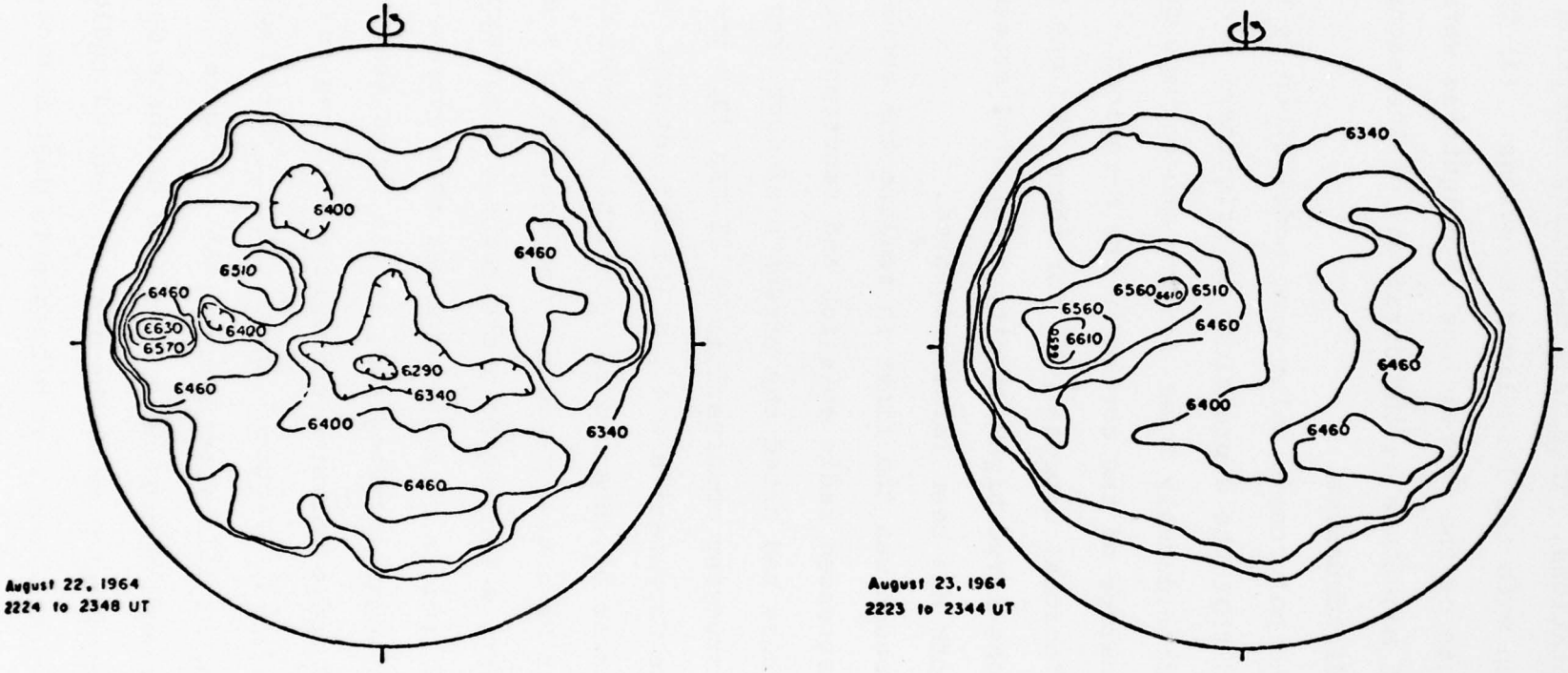

Fig. 1 Radio maps at 3.3 mm-λ showing depressions in brightness temperature near the center of the solar disk. These depressions were not associated with H-alpha filaments (adatped from Simon, 1965).

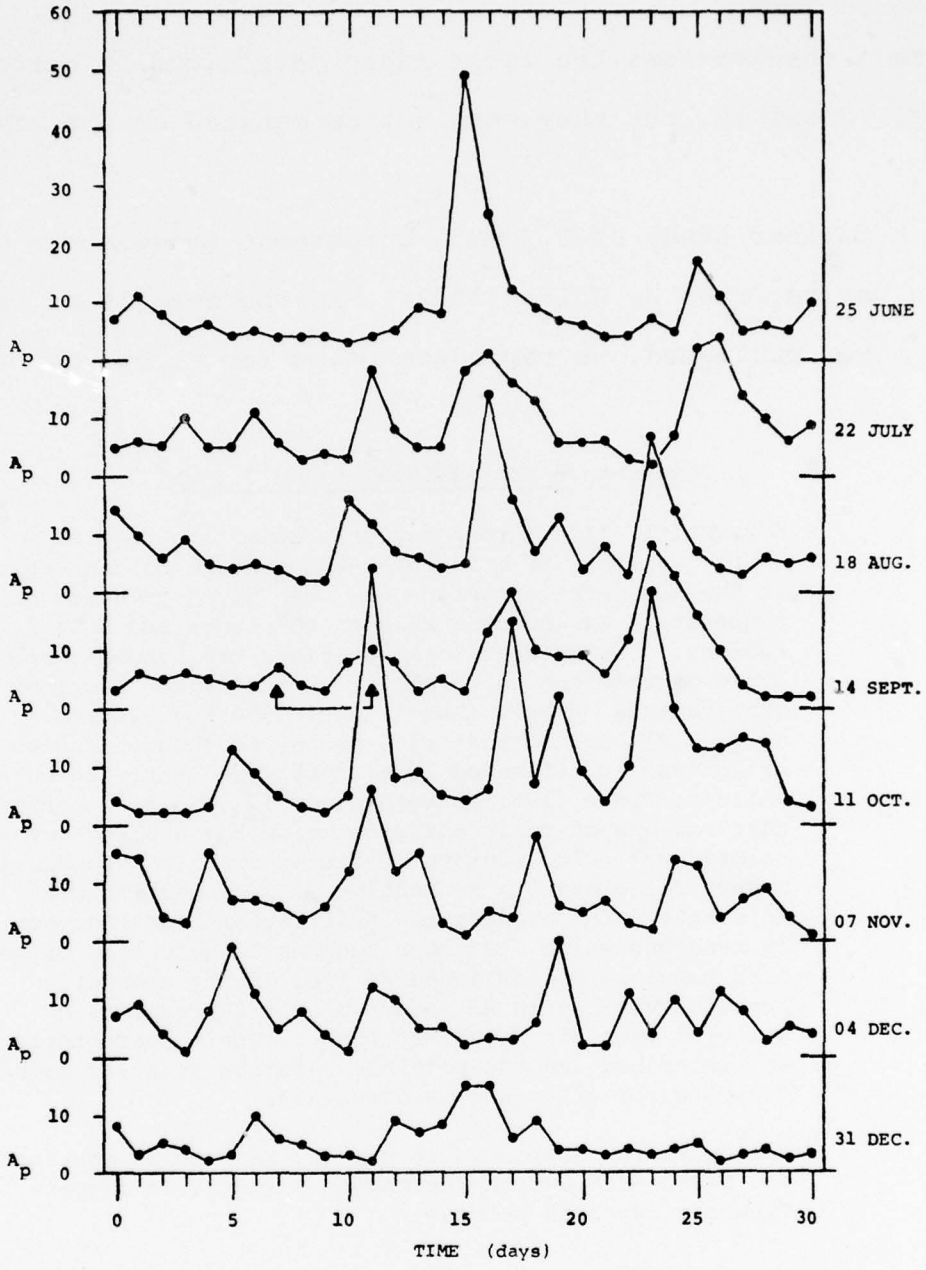

Fig. 2 The variation of A_p is shown during eight solar rotations in 1964. The date of the last A_p value in each 30 day long row of data is shown along the right-hand ordinate. The central meridian passage of the depression in brightness temperature of Figure 1 and the small recurrent geomagnetic disturbance four days later are indicated by the connected arrows near the center of the plot. The A_p data are from volumes 69 and 70 of J.G.R.

3.3 mm λ observations the first radio detections of coronal holes? Possibly, but they were not recognized at the time as such.

A further study of 3.3 mm λ brightness temperature depressions was reported by White (1972). As the details of the study were never published, we reproduce below the referenced abstract.

Temperature Depressions at λ = 3.3 mm.

K.P. White, III, Airospace Corporation in U.C.L.A. - In the analysis of brightness-temperature contour maps of the sun, most attention has been given to areas of temperature enhancement related to plages and active regions. The present work describes brightness-temperature depressions which appear on the maps. Previous observations by U.V. Khangil'din (1964 Sov. Astron. - AJ 8, 234) claimed that all regions of reduced radio-brightness are situated above dark quiescent filaments, while M. Simon (1965 Astrophys. J. 141, 1513) reported that regions of radio emission below the average correlated well with regions of little or no longitudinal magnetic field, with no mention of a connection with filaments. The present analysis reveals some temperature depressions which lie above regions largely free of measured magnetic fields and also free of any absorption material visible in Hα. Some of the depressions are followed over six solar rotations. Their characteristics are described and the possible relation to solar magnetic field sector structure is discussed.

This work was supported in part by NASA under contract No. NAS 2-6346 and the Aerospace Corporation company financed research program.

With the advent of telescope systems in space capable of recording images of the sun at EUV and soft X-Ray wavelengths, coronal holes became directly observable. Direct comparisons could then be made between these heliograms and the radio maps. Dulk and Sheridan (1974) have reported observations at 80 MHz

(3.75 m-λ) and 160 MHz (1.8 m-λ) using the Culgoora radio-heliograph. In comparisons with the NASA GSFC OSO-7 284 Å heliograms, they found depressions in the radio emission (amounting to 10-30% of the normal values) corresponding in location with, and rotating with coronal holes. They conclude that the radio manifestation of coronal holes must be due to a decrease in both the coronal temperature and density within the hole.

Fürst and Hirth (1975) have reported an observation at 10.7 GHz (2.8 cm-λ) using the Bonn 100-m telescope. They found a depression in the radio emission (amounting to 3-4% of the normal values) which "at least partly corresponds to a coronal hole".

Wefer et al. (1976), and Wefer and Bleiweiss (1976) have reported observations at 15.3 GHz (2.0 cm-λ) and 35 GHz (8.6 mm-λ) using the 18.3-m telescope of the La Posta Astrogeophysical Observatory. In comparisons with the NASA GSFC OSO-7 284 Å heliograms, they found areas of enhanced radio emissions (amounting to 1-3% of the central disk quiet sun brightness temperature). These areas were shown to correspond in location and shape with, and to rotate with, coronal holes.

Kundu and Liu (1976) have reported an observation at 85 GHz (3.5 mm-λ) using the NRAO 36 ft. telescope. They found an area of depressed radio brightness (amounting to 1-8% of normal values) which coincided with a coronal hole apparent on an X-Ray photograph obtained by a sounding rocket (Krieger et al., 1973). Unfortunately, this depression also coincides in position with (and has a shape strikingly similar to) a very

large Hα filament (Solar Geophysical Data, 1971).

Dulk et al. (1977) have compared EUV data with radio data at three wavelengths for coronal hole CH1 during its July August 1973 disk passages. They point to a discrepancy in the observations since they found no reasonable choice of the three parameters of their solar model which gave agreement between the radio and EUV data. Their study suggests the possibility that the radio brightness temperatures obtained for coronal holes are too small.

Shibasaki et al. (1977 and 1978) have presented observations at 3.75 GHz (8.0 cm-λ) with the Toyokawa radioheliograph. They found a region of depressed radio emission (amounting to approximately 27% of normal quiet values) which persisted for three solar rotations, was accompanied by a high-speed solar wind stream, and caused recurrent geomagnetic storms. Using a three component solar atmosphere model they concluded that the reduced radio emission was the result of a slightly reduced coronal temperature and a considerably reduced pressure in the coronal hole as compared with the quiet corona outside the hole.

More recently Wefer and Papagiannis (1977a) have combined data at nine radio wavelengths in the range 0.86 cm to 375 cm to determine the characteristic radio spectrum of coronal hole CH1. The spectrum was assembled from observations made during the May, June, and July 1973 disk passages of CH1. The observation of enhanced radio emission from coronal holes at 2.0 cm-λ mentioned above has been verified by near-simultaneous measurements made with the Haystack antenna in Massachusetts and the

La Posta antenna in California (Wefer and Papagiannis, 1977b). Coronal hole observations made with large single dish antennas have been extended to wavelengths of 11.5 cm and 21 cm by Papagiannis and Wefer (1977a, 1977b, 1978) using the Arecibo radiotelescope.

In addition to these two-dimensional observations, a number of researchers have reported one-dimensional (interferometer) observations of coronal holes. Chiuderi-Drago (1974) made observations at 408 MHz (73 cm-λ) with the Nancay interferometer. At 408 MHz the coronal hole shows up as a depression in radio emission amounting to a decrease of approximately 20% of normal coronal values.

Lantos and Avingnon (1975) have concluded, from observations made also at 169 MHz with the Nancay interferometer, that the radio quiet sun determined from the lower envelope of the daily drift scans corresponds to the level of emission from coronal holes.

Covington (1977) has reported observations at 2.8 GHz (10.7 cm-λ) made with the Algonquin interferometer. From a comparison of drift scans of a coronal hole (which extended nearly from pole to pole at central meridian) with drift scans made during 1975 (when solar activity reached extremely low levels) he concludes also that the radio emission from coronal holes coincides with that of the quiet sun.

3. SOLAR RADIO MAPS AT 9.1 CM WAVELENGTH

Beginning in June 1962 and continuing through August 1973 a nearly complete set of daily radioheliograms at the 9.1 cm wavelength were obtained at the Radio Astronomy Institute of Stanford University (Graf and Bracewell, 1975). The current study concerns only the last four months of these observations which overlap in time with the American Science and Engineering's S-054 experiment on the ATM (May through August 1973, Carrington rotations 1601-1605).

Details of the design and operation of the 9.1 cm radioheliograph have been given by Bracewell and Swarup (1961) and by Graf and Bracewell (1975); hence, the discussion here will be brief. The antenna used for the observations is composed of two equatorially-mounted, 16-element Christiansen arrays of 3 m (10 ft) diameter paraboloids, each array being 114 m in length. The half power contour of the antenna beam is elliptical, the east-west dimension being 3.1 arc min at the celestial meridian where the solar observations were made. The north-south dimension of the half power contour depends on the declination of the Sun and varies from 3.1 arc-min in summer to nearly 6.0 arc-min in winter. The central disk quiet sun brightness temperature is approximately 3.0×10^4 K at 9.1 cm-λ.

The data for a map were collected by making a number of drift scans of the Sun near local noon at declinations separated by $0.1130R_o \simeq 1.8$ arc min (R_o is the optical semi-diameter of the solar disk) and measuring the antenna temperature along each scan intervals of $0.1017R_o \simeq 1.6$ arc min. These observations

were made daily between 20:00 and 21:00 UT and resulted in a grid of antenna temperatures with 21 rows and 25 columns. The temperatures were corrected for receiver gain changes using calibrations made before and after the scans and assuming that the gain drifted linearly with time. The grid of points was rotated by the amount of the solar "P-angle" so that the solar rotation axis would be vertical, the required interpolation being done by the six point bivariate interpolation formula. The 21 by 25 grid of readings was normalized so that the flux density of the whole Sun (compute by summing the temperatures and taking into account the antenna beam solid angle) was equal to the absolute measurement made the same day at 10.7 cm-λ by the National Research Council, Ottawa, Canada. No adjustment was made for the difference in wavelength. The final readings were expressed in units of 1000 K. For the maps which appeared in Solar Geophysical Data these temperatures were divided by five and rounded to the nearest integer. For the study presented here we have used the temperature grids as available on magnetic tape with temperatures in units of 1000 K (Graf and Bracewell, 1975).

4. SYNOPTIC CHARTS AND 9.1 CM WAVELENGTH

A few rather crude synoptic charts of 9.1 cm solar radio emission were presented by Roosen (1969). More recently Graf and Bracewell (1975) have presented synoptic charts for each solar rotation from June 1962 through August 1973 (Carrington roations 1455 - 1605). In these charts emphasis was placed on

active regions, the lowest contoured level being 4.0×10^4K. Because the central disk quiet Sun brightness temperature is 3.0×10^4K and because coronal holes manifest themselves as depressions in radio emission at this wavelength (Wefer and Papagiannis, 1977a), these synoptic charts are not useful for the study of coronal holes.

The synoptic charts of 9.1 cm-λ radio emission presented in this study were constructed as follows. From each radioheliogram during the period 4 May 1973 through 31 August 1973, we extracted the central column (the central meridian temperature from each row) from the temperature grid. These columns were assembled into five new temperature grids (21 rows by 30 columns with time increasing to the left) covering the five Carrington rotations during the period. The temperatures were multiplied by (100.0/30.5) to bring the quiet Sun level up to approximately 100. Contouring these grids yielded the synoptic charts shown below.

This technique is much simpler than that used by Graf and Bracewell (1975) and somewhat simpler even than the one used by Roosen (1969). The charts so produced contain only information on the appearance of the Sun at central meridian. They are thus suitable only for studies of long-lived features such as coronal holes. We constructed a few charts using the radioheliogram columns to the left and to the right of central meridian charts. These charts showed the same general features as the central meridian charts, but differed somewhat in the finer details.

The computer program used to contour the map grids was adapted from the one used at La Posta Astrogeophysical

Observatory. In traversing the temperature grid at a particular contour level, "high ground" is kept always on the right. Ambiguities such as those that occur at saddle points are resolved by the program always attempting first to make a right turn. Linear interpolation is used in determining where along a row or column the contour line should cross. These points are connected sequentially by straight line segments. In order to make the direction of decreasing temperature readily apparent, short tic marks are placed on the low side of the contour line at the midpoint of each line segment.

The interval between contours is not constant on these maps. Rather it is varied, using a larger interval where the temperature gradient is high and the smaller contour intervals where the surface is nearly flat. Contour labels are in units of percent of the central disk quiet Sun temperature. Given below are the levels at which contours are drawn on the charts. The underlined levels are the ones labelled on the charts: 0, 20, 40, 60, 80, 90, 100, 110, 125, 150, 200, 500, 100. 1500, 2000, 2500,

In addition to the contour lines, the locations of the solar equator and the northern and southern photospheric limbs are shown. The charts are continued into the corona beyond the northern and southern limbs. Heliographic latitude scales are given at both the right-hand and left-hand edges of the synoptic charts. A Carrington longitude scale is given at the top. At the bottom of each chart are given the Carrington rotation number and the dates of the maps used for each column of the temperature grid. The small triangles indicate the location of each column and mark 20:00 UT on the date shown.

Coronal holes are shown on the synoptic charts as shaded regions. The boundaries of coronal holes CH1 through CH6 were taken from Nolte et al. (1976b). Some additional boundaries were taken from Bohlin and Rubenstein (1975). In drawing the boundaries on synoptic charts we have relied heavily on the work of Hanson and Roelof (1978), who have made a similar superposition.

5. THE SYNOPTIC CHARTS

The synoptic chart of 9.1 cm solar radio emission for Carrington rotation 1601 is shown in Figure 3. The radio data cover the period 4 May through 2 June 1973; however, the S 054 X-ray photographs did not begin until 28 May. The thin shaded region in Figure 3, which extends from the north limb to almost the south limb near Carrington longitude zero, is coronal hole CH1. Accompanying CH1 but shifted slightly eastward is a depression in radio emission extending from the north limb to latitude N 20°. The depression is overwhelmed by enhancements in radio emission associated with McMath plage regions 12362 and 12363, but manages to show itself again around latitude S 25°.

The correspondence between the X-Ray coronal hole and the 9.1 cm radio depression is not particularly impressive in this case; however, it should be noted that the E-W extent of the hole is smaller, along most of its length, than the half power beam-width of the antenna. The other X-Ray holes are either too close to the limb to be detectable, or are obscurred by the substantial side-lobe effects near active regions.

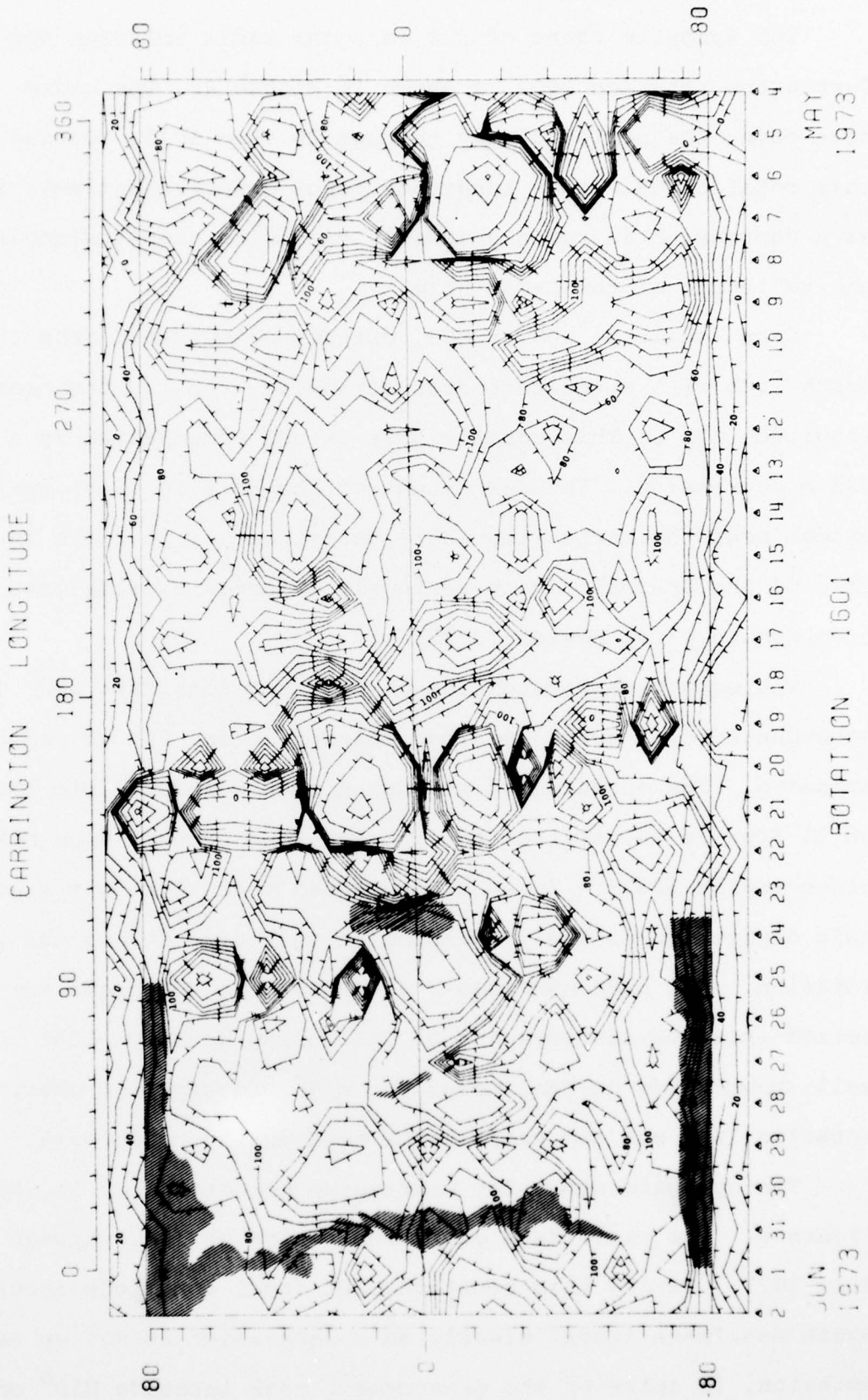
CARRINGTON LONGITUDE
0
90
180
270
360
80
0
-80
ROTATION 1601
MAY 1973
JUN 1973

FIGURE 3

The synoptic chart of 9.1 cm solar radio emission for Carrington rotation 1602 is shown in Figure 4. The radio data cover the period 31 May through 29 June 1973. During this rotation CH1 (near longitude zero) clearly manifests itself as a depression in radio emission, extending almost along the entire length of the X-Ray hole.

Near longitude 90° is CH3, extending southward from the north limb with a separate area straddling the equator near longitude 120°. This coronal hole is not accompanied by a radio depression. The E-W extent of the hole is quite small, except near the north limb where, unfortunately, it falls in an area of the synoptic chart seriously affected by side-lobe effects from McMath plage region 12397.

The equatorward extension of CH5 near longitude 260° is accompanied by a substantial depression in the 9.1 cm radio emission. The enhancement extending southwestward into the hole on 11 June is an artifact due to side-lobe effects from McMath plage region 12379. It should be noted that there was a considerable depression in radio emission in this area during the previous rotation. The NASA GSFC OSO-7 284 Å spectroheliograms for the period indicate the presence of CH5 during Rotation 1601 as well. Other X-Ray coronal holes shown on the synoptic chart for rotation 1602 are too small to be seen in the radio data.

The synoptic chart for Carrington Rotation 1603 is shown in Figure 5. The radio data cover the period 28 June through 27 July 1973. During this rotation, CH1 (near longitude zero) again manifests itself clearly as a depression in 9.1 cm radio emission, in spite of the enhancement near latitude N10° on

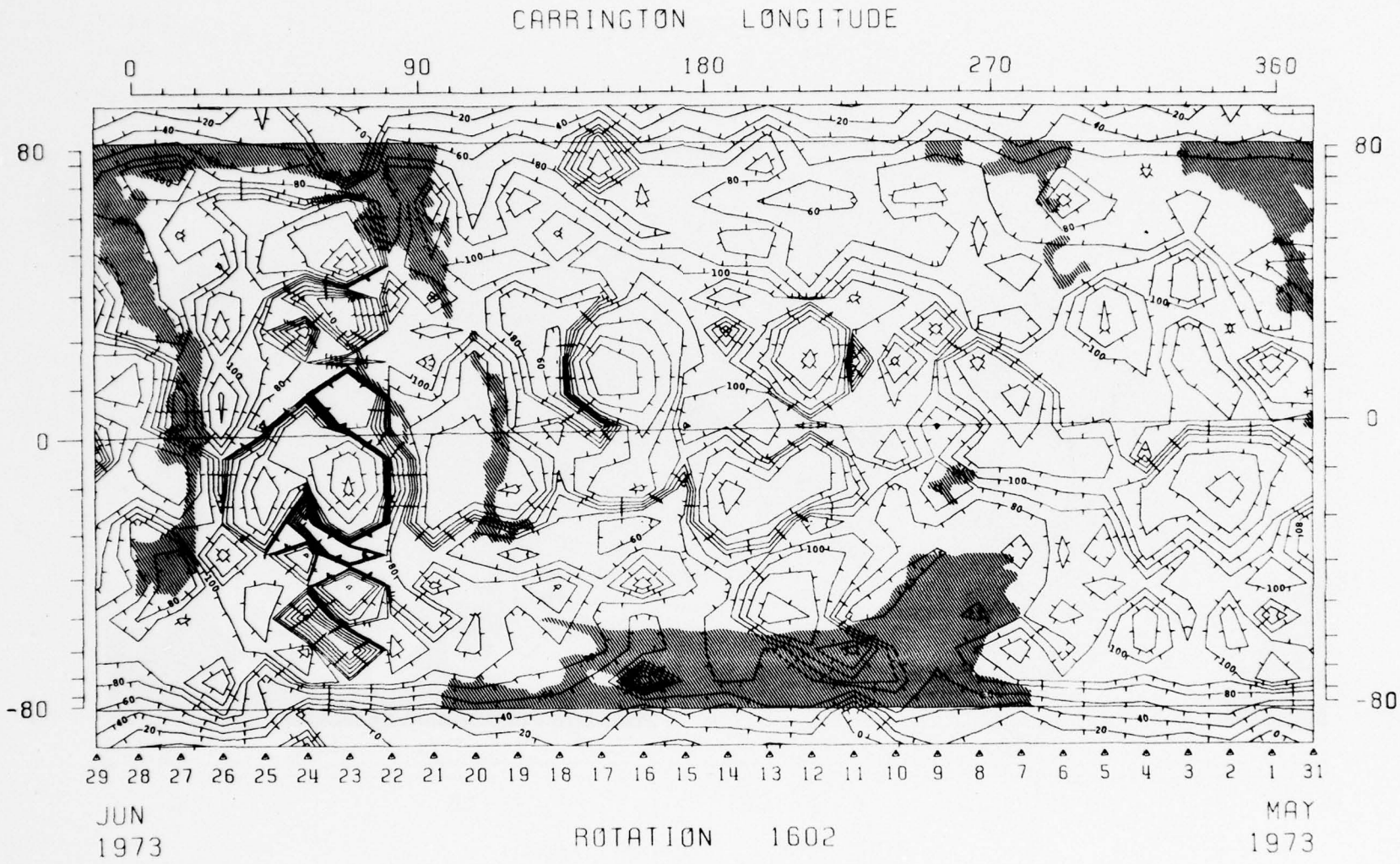
CARRINGTON LONGITUDE
0
90
180
270
360
80
0
-80
29 28 27 26 25 24 23 22 21 20 19 18 17 16 15 14 13 12 11 10 9 8 7 6 5 4 3 2 1 31
JUN
1973
ROTATION 1602
MAY
1973

FIGURE 4

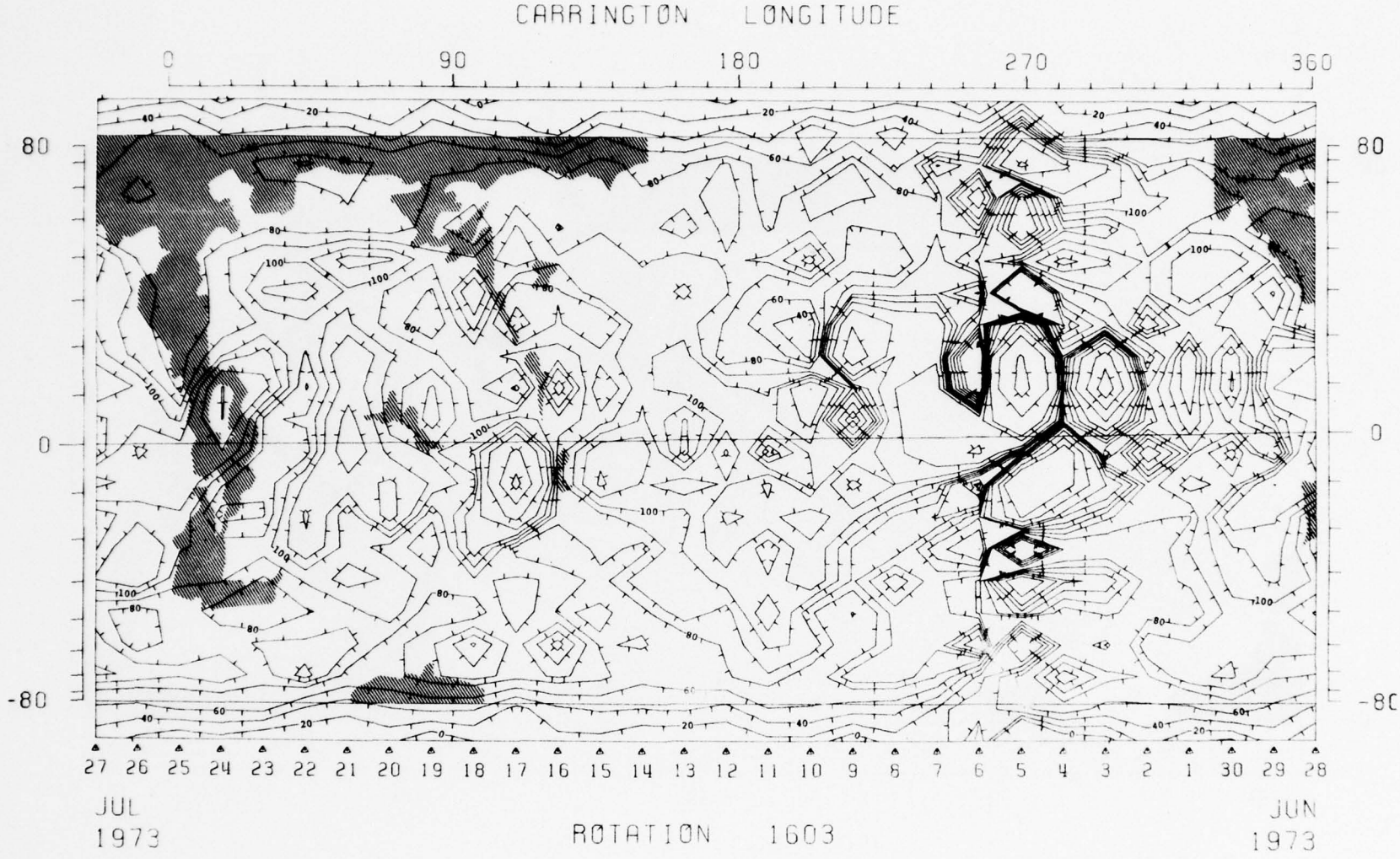
CARRINGTON LONGITUDE
0
90
180
270
360
80
0
-80
27 26 25 24 23 22 21 20 19 18 17 16 15 14 13 12 11 10 9 8 7 6 5 4 3 2 1 30 29 28
JUL
1973
ROTATION 1603
JUN
1973

FIGURE 5

24 July due to McMath plage region 12451. Coronal holes CH2 and CH3 were, by this rotation, too small to cause noticable depressions in the radio data.

The synoptic chart for Carrington Rotation 1604 is shown in Figure 6. The radio data cover the period 25 July through 23 August 1973. Coronal Hole 1 is not convincingly seen on this chart. The enhancement near longitude 10°, latitude $N55^{\circ}$ is a side-lobe effect from an active region which crossed the central meridian on 23 August (see Figure 7). Nevertheless, based on its appearance during rotation 1603, one would have expected to see a more pronounced depression in 9.1 cm radio emission accompanying an X-Ray hole of this size.

Again CH2 and CH3 are too small to be seen. The radio depression accompanying the unnamed equatorward extension of the south polar coronal hole (4-12 August) is also not particularly convincing. The synoptic chart for Carrington rotation 1605 is shown in Figure 7. The radio data cover the period 21 August through 31 August when the program of daily 9.1 cm radio observations ended. There were no additional coronal holes observed during this ten day period.

6. CONCLUSIONS AND DISCUSSION

From the above examination of the 9.1 cm synoptic charts it can only be concluded that sometimes coronal holes are observable in the Stanford data, and sometimes they are not. At least two factors determine whether a particular hole is detectable:

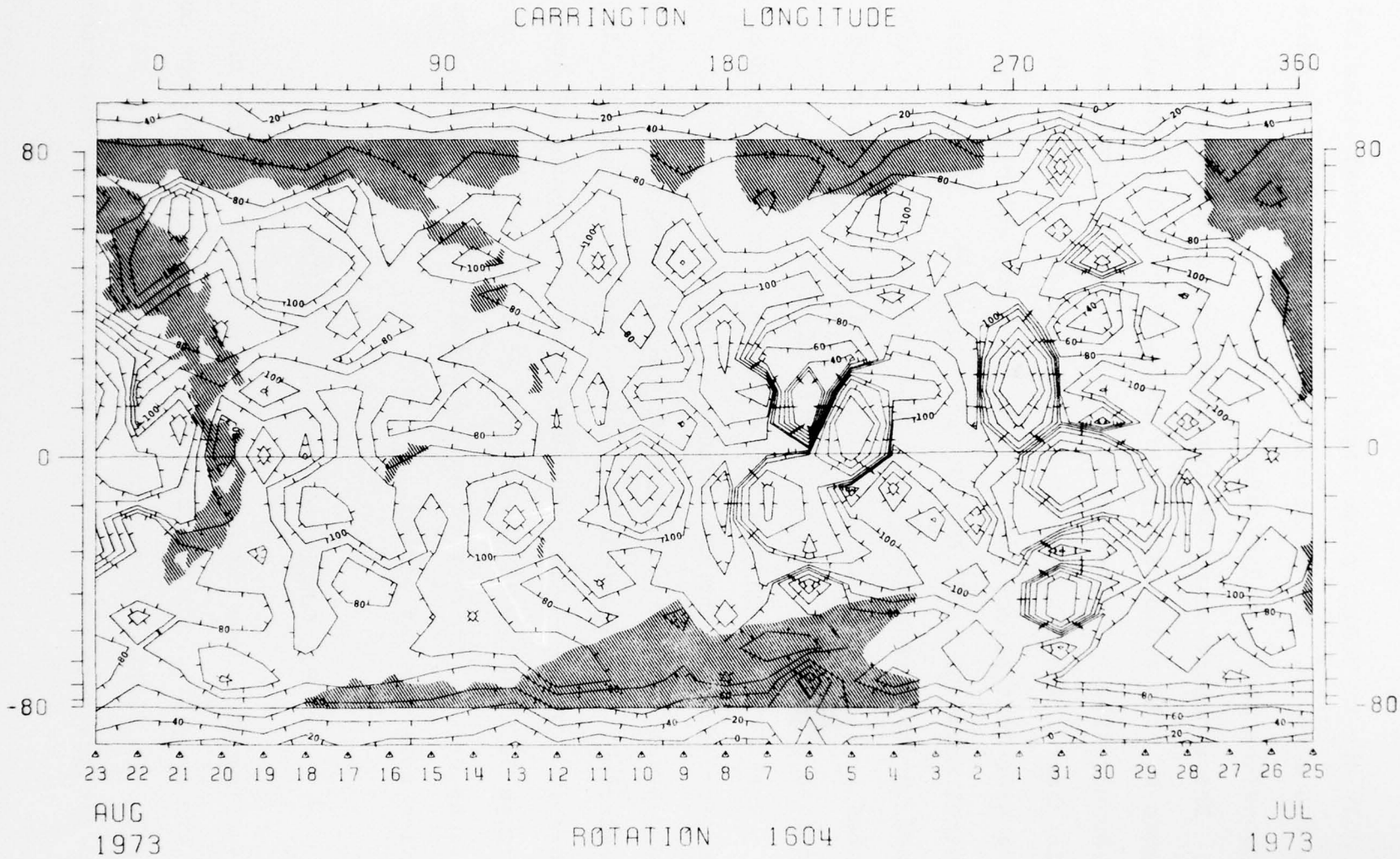
CARRINGTON LONGITUDE
0
90
180
270
360
80
0
-80
23 22 21 20 19 18 17 16 15 14 13 12 11 10 9 8 7 6 5 4 3 2 1 31 30 29 28 27 26 25
AUG
1973
ROTATION 1604
JUL
1973

FIGURE 6

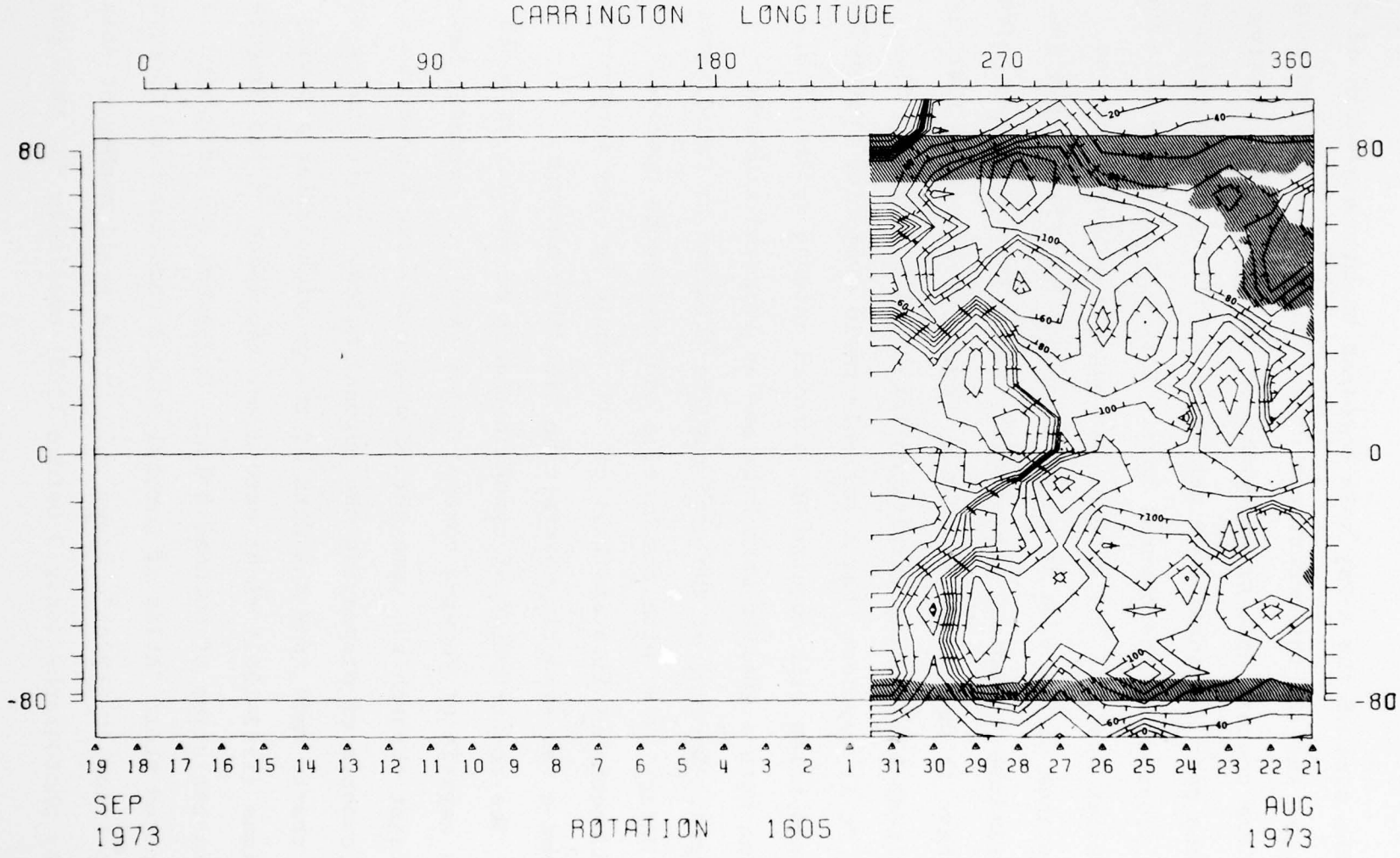
CARRINGTON LONGITUDE
0
90
180
270
360
80
0
-80
19 18 17 16 15 14 13 12 11 10 9 8 7 6 5 4 3 2 1 31 30 29 28 27 26 25 24 23 22 21
SEP
1973
ROTATION 1605
AUG
1973

FIGURE 7

(1) the size of the X-Ray hole compared to the beam-width of the antenna, and (2) the occurrence of active regions located either near the coronal hole or elsewhere on the solar disk. Active regions near a coronal hole can cause a filling of the radio depression produced by the coronal hole. Active regions anywhere on the solar disk, if hot enough, can cause a confusion in the appearance of the area in which a coronal hole is located due to sidelobe effects. The spatial extent which sidelobe effects can have is dramatically shown by McMath plage region 12417 near longitude 270° during Carrington Rotation 1603 (Figure 5).

It is apparent that a reliable radio detection system for coronal holes will require an improved antenna system, i.e., one having both a smaller main beam and an improved sidelobe pattern. Because of the good results obtained by Papagiannis and Wefer (1978) with the Arecibo radiotelescope operated at wavelengths of 11.5 and 21.1 cm, it would be very interesting to see a few synoptic charts made with this antenna.

The construction of synoptic charts of the 9.1 cm radio data capable of showing coronal holes should be extended backward at least through the time period when OSO-7 284 Å spectroheliogra are capable of displaying the coronal holes. Additionally synoptic charts made from the data of the previous solar activity minimum (1963-1965) might extend our knowledge of the temporal characteristics of coronal holes. Underwood and Broussard (1977) prepared their "Atlas of Coronal Hole Boundaries From Observations Made Prior to Skylab", based only on the small number of solar X-Ray photographs (only 3 before 1965) available for this period.

These results can be significantly strengthened through a careful search for coronal holes in the 9.1 cm synoptic chart data (especially in the 1962-1965 period of low solar activity) in the manner employed for the first time in this report.

7. REFERENCES

Bracewell, R.N. and Swarup, G.: 1961, IRE Transactions on Antennas and Propagation, Vol. AP-9, No. 1, 22-30, January.

Bohlin, J.D. and Rubenstein, D.M.: 1975, Report UAG-51, World Data center A for Solar-Terrestrial Physics, Boulder, Colorado, 21 pages, November.

Chiuderi-Drago, F.: 1974, paper presented at the Skylab Conference, Florence, Italy, March 21-22, 1974.

Covington, A.E.: 1977, Solar Physics, 54, 393-402.

Dulk, G.A. and Sheridan, K.V.: 1974, Solar Physics, 36, 191-202.

Dulk, G.A., Sheridan, K.V., Smerd, S.F. and Withbroe, G.L.: 1977, Solar Physics, 52, 349-367.

Fürst, E. and Hirth, W.: 1975, Solar Physics, 42, 157-161.

Graf, W. and Bracewell, R.N.: 1975, Report UAG-44, World Data Center A for Solar-Terrestrial Physics, Boulder, Colorado, 183 pages, May.

Hanson, J.M. and Roelop, E.C.: 1978, Johns Hopkins University, Applied Physics Laboratory Report JHU/APL 78-05, 22 pages, May.

Krieger, A.S., Timothy, A.F. and Roelof, E.C.: 1973, Solar Physics, 29, 505-525.

Kundu, M.R. and Liu, Sou-Yang: 1976, Solar Physics, 49, 267-269.

Lantos, P. and Avignon, Y.: 1975, Astronomy and Astrophysics, 41, 137-142.

Maer, K. and Dessler, A.J.: 1964, J.G.R.,68, No. 24, 6361-6370, 15 Dec.

Neupert, W.M. and Pizzo, V.: 1974, J.G.R.,79, No. 25, 3701-3709, 1 Sept.

Nolte, J.T., Krieger, A.S., Timothy, A.F., Gold, R.E., Roelof, E.C., Vaiana, G., Lazarus, A.J., Sullivan, J.D. and McIntosh, P.S.: 1976a, Solar Physics,46, 303-322.

Nolte, J.T., Krieger, A.S., Timothy, A.F., Vaiana, G.S. and Zombeck, M.V.: 1976b, Solar Physics,46, 291-301.

Papagiannis, M.D. and Wefer, F.L.: 1977a, AAS Bulletin,9, 4 II, 617.

Papagiannis, M.D. and Wefer, F.L.: 1977b, EOS,59, No. 4, 367-368, April.

Papagiannis, M.D. and Wefer, F.L.: 1978, Nature,273, No. 5663, 520-522, 15 June.

Parker, E.N.: 1963, Interplanetary Dynamical Processes, Interscience Publishers, New York.

Roosen, J.: 1969, Solar Physics,7, 448-462.

Sheeley, N.R., Harvey, J.W. and Feldman, W.C.: 1976, Solar Physics,49, 271-278.

Shibasaki, K., Ishiguro, M., Enome, S. and Tanaka, H.: 1977, Solar Terrestrial Environmental Research in Japan,1, 1-2, 1 Dec.

Shibasaki, K., Ishiguro, M., Enome, S. and Tanaka, H.: 1978, Publications of the Astronomical Society of Japan (in press).

Simon, M.: 1965, Astrophysical Journal, 141, No. 4, 1513-1522.

Snyder, C.W., Neugebauer, M. and Rao, V.R.: 1963, J.G.R., 68, No. 24, 6361-6370, 15 Dec.

Solar-Geophysical Data: 1971, Number 3.7 - part I (prompt reports), 65.

Solodyna, C.V., Krieger, A.S. and Nolte, J.T.: 1977; Solar Physics, 54, 123-134.

Underwood, J.H. and Broussard, R.M.: 1977, Aerospace Corporation Report No. ATR-77 (7405)-2.

Wefer, F.L., Bleiweiss, M.P. and Hurst, M.D.: 1976, Megatek Corp. report R2005-031-F01, 1 July.

Wefer, F.L. and Bleiweiss, M.P.: 1976, AAS Bulletin, 8, No. 2, 338-339.

Wefer, F.L. and Papagiannis, M.D.: 1977a, AFGL-TR-77-0292, Dec.

Wefer, F.L. and Papagiannis, M.D.: 1977b, AAS Bulletin, 9, 4 II, 617.

White, K.P.: 1972, AAS Bulletin, 4, 3II, 395.